ISBN: 978-3-95450-234-9 ISSN: 2673-5504 doi:10.18429/JACoW-SRF2023-TUPTB059

INFN LASA EXPERIMENTAL ACTIVITIES FOR THE PIP-II PROJECT

M. Bertucci*, M. Bonezzi, A. Bosotti, D. Cardelli, E. Del Core, F. Fiorina, A. T. Grimaldi, L. Monaco, C. Pagani, R. Paparella, D. Sertore, M. Zaggia
INFN Milano - LASA, Segrate, Italy

Abstract

INFN LASA is upgrading its vertical test facility to allow high-Q measurements of the PIP-II LB650 SRF cavities. Such facility is equipped with a wide set of diagnostics for quench, field emission and magnetic flux expulsion studies and will offer a better understanding of cavity performance. At the same time, R&D on LB650 cavity prototypes is ongoing, in order to optimize the overall processing as well as the cavity Jacketing in view of the forthcoming series production with industry. This paper reports on the overall status of these experimental activities.

INTRODUCTION

The Fermilab Proton Improvement Plan II (PIP-II) Linac [1] is designed to provide an 800 MeV H- beam. This beam will then undergo injection into the Booster Ring and subsequently be transferred to the Main Injector ring, ultimately enabling the generation of a powerful 1.2 MW beam. This high beam power is crucial for conducting the LBNF and DUNE neutrino physics experiments, which hold significant implications for scientific research.

A vital aspect of the PIP-II linac is the low-beta (LB) section, for which INFN LASA has taken responsibility. The task involves the production of 40 superconducting cavities operating at 650 MHz with a β value of 0.61 [2]. To ensure optimal performance within the machine, these cavities must meet specific requirements, including an E_{acc} of 16.9 MV m^{-1} and a Q_0 value of at least $2.4 \cdot 10^{10}$ at the operating field. Achieving these high-performance standards necessitates the development of a "high-Q" surface recipe. Extended research has been conducted to explore various recipes in order to identify the most optimal solution in terms of cavity performance and mechanical stability. It is for instance crucial to ensure that target values for Q_0 and E_{acc} are maintained throughout the entire production process, from before the Helium tank Jacketing to the installation in the cryostat. Any significant drifts in the operating frequency and cavity field flatness must be minimized. Meeting these stringent requirements has prompted the development of an optimized cavity processing sequence that is suitable in the context of a large-scale series production.

CURRENT STATUS OF PIP-II LB650 CAVITY PROTOTYPES

INFN, in collaboration with the company Zanon Research & Innovation Srl., manufactured a total of 7 PIP-II LB650 prototypes. Among them, 5 are single-cell cavities, while the remaining 2 are multicell cavities. As part of the collaboration, 2 cavities were shared with FNAL [3]. One of the single cell cavities, named B61S-EZ-001, underwent a high-Q recipe based on N-doping. The process included a 160 µm bulk EP, followed by a 900 °C HT for 3 hours + 2/0 N-doping at 800 °C. The cavity was then subjected to a final EP. The second shared cavity, the multicell cavity named B61-EZ-001, underwent a baseline treatment. This involved a 160 µm bulk EP, a 800 °C HT for 2 h, a final EP and a 120 °C 48 h bake. Eventually the cavity was jacketed with helium tank. In both cases, the project goals were successfully met.

Single cell cavity B61S-EZ-002 and multicell cavity B61-EZ-002 were surface-treated at the company under the supervision of INFN, with the goal of optimizing the already operating infrastructures to the specific case of LB650 cavities, and then to demonstrate the feasibility of high-Q treatments of LB650 cavities in the industrial context. Two other single cell cavities will be surface processed in the future with high-Q recipes which are still under definition.

Cavity B61S-EZ-002

The single cell cavity B61S-EZ-002 played a crucial role in adapting the Electropolishing plant to the different size and geometry of PIP-II LB650 cavities. The treatment parameters were carefully optimized to enhance smoothness, removal rate and iris/equator removal ratio [4]. To increase the removal rate at the equators, aluminum cathode enlargements were installed in correspondence of the center of cells. Subsequently, the same cavity was then utilized to test a baseline treatment sequence that will serve as a reference for future high-Q treatments. This sequence involved a 150 µm bulk EP, a 800 °C HT for 2 h, a 25 µm cold final EP and a 120 °C 48 h bake. In the final EP treatment the "cold" regime was employed. The average temperature on cavity surface is maintained below 12 °C, ensuring a smoother surface finishing at the end of the treatment. The vertical test results at 2 K are affected by poor flux expulsion regime due to the slow cooldown rate of LASA-INFN cryostat (approximately 1 K min^{-1} at the transition temperature corresponding to a 82% measured trapped flux efficiency). Despite this, a $Q_0 = 2 \times 10^{10}$ was achieved at the target E_{acc}=16.9 MV m^{-1} [5]

Cavity B61-EZ-002

The multicell cavity B61-EZ-002 underwent the mid-T bake recipe. The treatment involved a 150 µm bulk EP, followed by a 800 °C HT for 2 h, a 5 µm cold final EP and a 300 °C 3 h bake. This last step took place in the same

* michele.bertucci@mi.infn.it

ISBN: 978-3-95450-234-9 ISSN: 2673-5504 doi:10.18429/JACoW-SRF2023-TUPTB059

furnace used for high-temperature annealing in UHV conditions, with a pressure of approximately $4 \cdot 10^{-7}$ torr. The effect of such treatment is the oxygen redistribution within the subsurface layer. This redistribution plays a crucial role in preventing additional losses caused by hydride segregation [6]. Subsequently, the cavity was exposed to air allowing the regrowth of the Nb_2O_5 layer.

During the first test at 2 K the cavity exhibited field emission above 20.8 MV m^{-1}. This led to a sudden increase in radiation level and a Q-degradation. In a subsequent power rise, the onset of radiation decreased to 14 MV m^{-1}, accompanied by a simultaneous drop of the Q_0, until the cavity ultimately quenched at 23 MV m^{-1}. This behavior can be attributed to the irreversible activation of a field emitter induced by RF heating at high fields [5]. In this case, a $Q_0 = 1.9 \times 10^{10}$ was attained at the project goal $E_{acc} = 16.9$ MV m^{-1}. The final test results at 2 K for cavities B61S-EZ-002 and B61-EZ-002 are shown in Fig. 1.

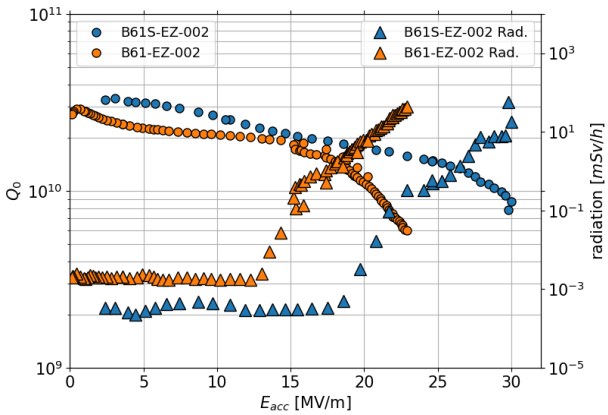

Figure 1: Q vs E_{accc} and radiation vs E_{acc} for Cavity B61S-EZ-002 and B61-EZ-002 at 2 K.

After the vertical test, the cavity was equipped with the FMS (field profile measurement system) which allows to measure cavity frequency spectrum and field flatness even outside a clean room while mantaining the cavity in clean conditions [7]. This setup allows for separate pumping-venting procedures in the cavity inner volume and in the Teflon tube in which the bead-pull measurement is conducted. Figure 2 shows the FMS setup installed on the beam tube flange.

The cavity was then equipped with a full set of diagnostics for measuring flux expulsion. This consists in 3 fluxgates which are oriented towards the three cavity axis, so to measure the trapping flux efficiency for the cryostat residual magnetic field, and a set of temperature sensors mounted at cavity top, bottom and middle cell equators so to measure the temperature gradient at the transition temperature. Figure 3 shows cavity B61-EZ-002 fully integrated with diagnostics. Finally, the cavity was integrated with the Helium tank. The evolution of field flatness and fundamental mode frequency during different steps of tank integration is shown in Fig. 4. All measurements were performed

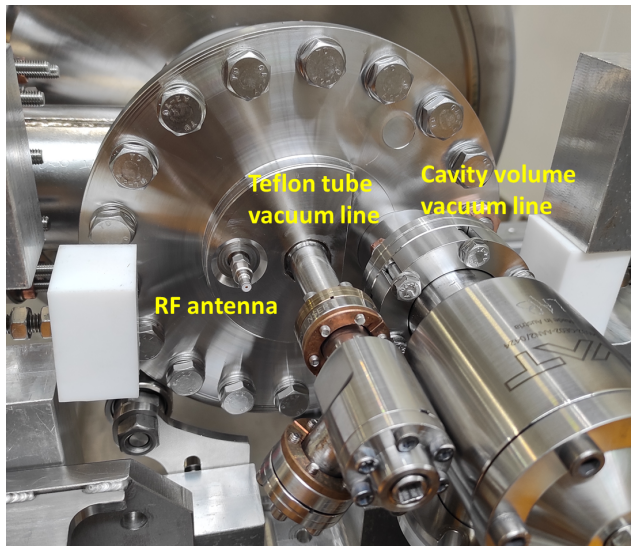

Figure 2: FMS setup installed on cavity B61-EZ-002.

with cavity inner volume in a Ar atmosphere and with the FMS Teflon tube installed. The overall effect of both is a 70 kHz shift with respect to the cavity frequency in vacuum. A significant field flatness change can be noticed after the welding of end-cups and bellow, which was promptly corrected by means of a field flatness fine tuning operation which fully recovered the previous value. The final value of 92.3% is above the required PIP-II target ($FF \geq 90\%$ after tank integration)

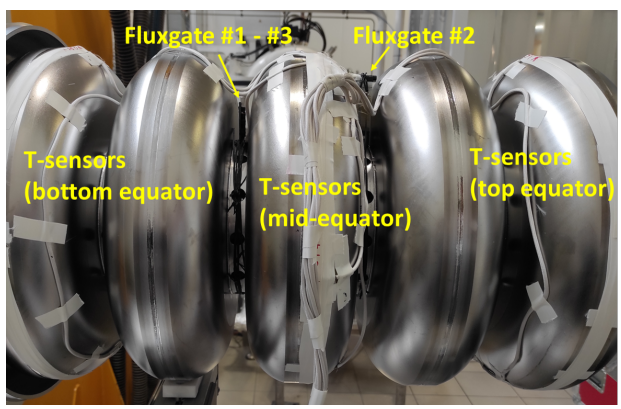

Figure 3: Cavity B61-EZ-002 with integrated diagnostics for flux expulsion studies.

A future vertical test of the dressed cavity is planned at LASA facility so to verify the effect of tank integration on cavity performance and to check the integrated diagnostics for flux expulsion.

LASA ACTIVITIES TOWARDS THE CAVITY SERIES PRODUCTION

While the prototyping phase is still ongoing, the strategy for cavity series production is now under definition. In synergy with FNAL, the experimental data so far collected with

ISBN: 978-3-95450-234-9 ISSN: 2673-5504 doi:10.18429/JACoW-SRF2023-TUPTB059

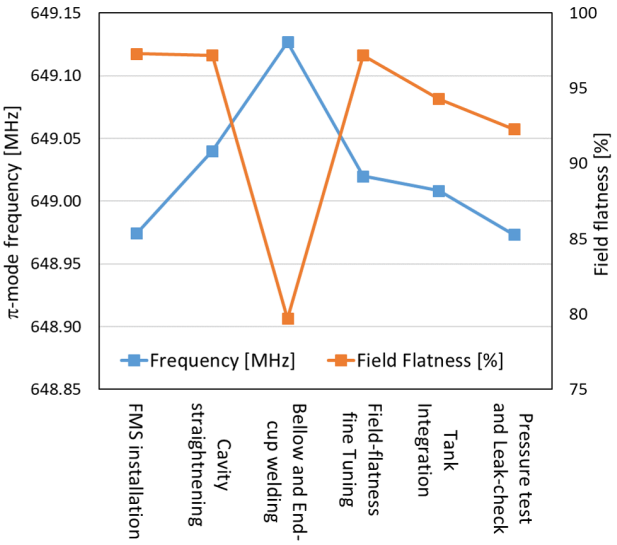

Figure 4: Evolution of accelerating mode frequency and field flatness during tank integration.

the prototype tests have been carefully analyzed and many conclusions have been already drawn.

Optimization of Cavity Surface Recipe

The mid-T bake recipe stands out as a promising option among various high-Q treatments because it eliminates the need for additional final EP to tune the impurity content to the desired level in the RF-active Nb layer. Recent experimental findings have shown that mid-T bake reduces the temperature-dependent BCS surface resistance, but it also leads to a parallel increase in residual resistance due to enhanced trapped flux sensitivity. To restore the magnetic flux expulsion properties of the material, annealing at temperatures equal or greater than 900 °C is necessary, but this may impact the mechanical stability of the cavity. Notably, recent findings [8] reveal that TESLA-type 1.3 GHz cavities mid-T baked at 300 °C exhibit a sensitivity of 1.5 nΩ mG^{-1} at low field, which is over three times higher that that achieved with ordinary 120 °C low temperature baking.

The impact of the slow cooldown conditions in the LASA-INFN cryostat on the mid-T baked cavity B61-EZ-002 was assessed assuming a conservative value of 1 nΩ mG^{-1} for trapped flux sensitivity. With an average residual field of $B \approx 6$ mG and a trapped flux efficiency $\eta \approx 80\%$, the residual resistance is calculated as $R_{t.f} = \eta \cdot S \cdot B = 4.8$ nΩ. Figure 5 shows the experimental Q_0 vs E_{accc} for Cavity B61-EZ-002 along with the theoretical Q_0 assuming full flux expulsion, namely subtracting $R_{t.f.} = 4.8$ nΩ from the experimental surface resistance, as $R_s(B=0) = R_{s,exp} - R_{t.f.} = \frac{G}{Q_{exp}} - R_{t.f.}$. This result is consistent with experimental results obtained for similar cavities in high flux expulsion conditions [9].
The ongoing optimization of treatment parameters extends to the Electropolishing (EP) plant as well. The same facility is intended for use in both warm and cold EP treatments, with a maximum temperature setpoint of 20 °C for cavity walls during warm EP and 12 °C during cold EP. Achieving the cold EP temperature set-point is made possible through the utilization of external water chillers [4]. Due to limitations in the available supply power, a supply voltage of 18 V was utilized in all INFN-LASA EP-treated LB650 prototypes. However, recent findings [10] have shown that a smoother surface finish can be achieved by employing a 23 V supply, which corresponds to the plateau region in the I-V polarization curve. There are plans to upgrade the power capabilities of the plant to enable EP in the full polishing regime. This upgrade is expected to further enhance the cavity Q-value by reducing dissipative mechanisms arising from surface roughness.

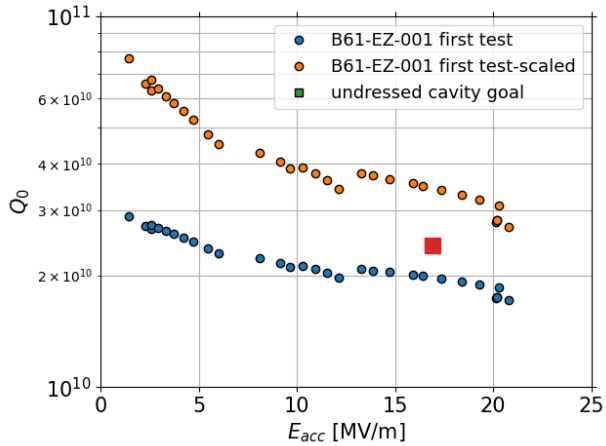

Figure 5: Q vs E_{accc} for cavity B61-EZ-002 at 2 K: experimental Q_0 and recalculated Q_0 assuming full flux expulsion with a 1 nΩ mG^{-1} sensitivity.

Definition of Cavity Production Cycle

The preparation of the technical specifications for the series production of LB650 PIP-II cavities at the industry is now ongoing. As for the case of ESS medium beta cavities production, three acceptance levels are foreseen in the production phase, each one including a list of controls and procedures to be fulfilled in order to proceed to the next level [11]. The first acceptance level (Al1) includes all the steps of cavity mechanical fabrication up to the electron beam welding. The second acceptance level (Al2) consists of all the fabrication steps before tank integration and therefore includes all the surface processing operation. Apart from the definition of minor details, the foreseen cavity recipe is as follows:

- bulk EP: 120 µm warm
- Heat treatment: 3 h at 900 °C in UHV
- Final EP: 20 µm warm + 20 µm cold
- mid-T bake: 3 h at 300 or 350 °C in UHV

The third acceptance level (Al3) consists of cavity tank integration and preparation for the cold RF test. Being no

ISBN: 978-3-95450-234-9 ISSN: 2673-5504 doi:10.18429/JACoW-SRF2023-TUPTB059

further surface treatments foreseen after tank integration, all the RF controls on field profile distribution and spectrum during preliminary operations before tank welding will be conducted by means of the previously mentioned FMS system so to protect the cavity inner volume from possible surface contamination.

After Al3 acceptance, cavity will leave the industry and will be shipped to the vertical test facility. The test of all series LB650 cavities is planned as a collaboration with DESY and will exploit AMTF infrastructure along a scheme already successfully adopted for the ESS project [12]. Two devoted inserts with two cavities each will be put in place to achieve the desired testing rate required during the series production. No active compensation of residual magnetic field will be realized while a consistent fast cool-down procedure will be defined by calibrating cryogenic data (e.g. outer wall temperatures, liquid helium mass-flow) with LB650 cavities prototypes equipped with diagnostics for temperature and magnetic flux expulsion, along the same lines of cavity B61-EZ-002.

As final step after cold test qualification, cavity will be shipped to CEA for integration into the cryomodule. Through an interplay among the different partners involved, the cavity shipment and testing configuration is being thoroughly discussed. A second access port to cavity vacuum has been designed in agreement with requirements of the string assembly team, hosting a separate all-metal CF16 valve and an UHV compliant sub-micrometric filter and so to provide a dedicated cavity venting line, safe from the standpoint of particle contamination and Q_0 degradation after string assembly. Overall, compatibility with activities planned upon string assembly at CEA has been secured.

Upgrade of LASA Vertical Test Facility

LASA vertical test facility is being upgraded in view of the tests of high-Q treated cavities. For the PIP-II LB650 testing purposes it can side DESY infrastructure by testing undressed cavities that require additional evaluation. LASA facility is indeed equipped with a wider set of cavity diagnostics allowing to better understand possible mechanisms of performance limitation.

LASA facility is equipped with a ISO4 clean room dedicated to cavity preparation for the test. The clean room hosts a High Pressure Rinsing station, which is currently being upgraded so to host PIP-II LB650 cavities, both undressed and tank-integrated. This will allow *in situ* cleaning of cavities displaying field emission during the vertical test.

The LASA cryostat has been extensively described in Ref. [13] At the present state, the LASA cryostat does not allow high cool-down rate at the transition temperature, but an upgrade is currently under way. From the point of view of Helium transfer dynamics, LASA cryogenic plant resides on dewars for the liquid helium mass-flow during cool-down and level build-up. Hence, the temperature drop rate at transition will be maximized through a devoted re-design of transfer lines, heaters and spraying nozzles around the cavity.

In the same time, an external field active compensation apparatus is currently under development. This setup is constituted by two Helmholtz coils and a central single coil that are operated with separate current sources. The coil position and currents must be set in such a way to obtain the lowest possible residual field at the cavity equator sites. Such optimization has been carried out considering coils center positions and currents as free parameters and then minimizing the analytical superposition of the coil fields and residual cryostat field at the equator sites. Figure 6 shows the results of such optimization procedure for a residual field of 10 mG. The optimum solution is found with a 22 cm distance between single coil and Helmholtz coils, a 0.26 A current for the two Helmholtz coils, and 0.14 A for the center single coil. The absolute value of residual field on cavity surface is calculated by means of the magnetostatic solver of CST Microwave Studio. The typical residual field at the cavity surface is less than 1 mG and never higher than 2 mG. This in turn would allow the reduction of $R_{t.f.}$ by a factor 10.

From the point of view of cavity diagnostics, second sound sensors (OST) and fast thermometry sensors are available to reconstruct possible quench events limiting the cavity operating gradient. An array of PIN photodiodes is installed inside the cryostat so to reconstruct field emission events, together with external detectors (proportional counter and NaI scintillator) allowing to measure X-ray dose rate and energy spectrum. The cavity flux expulsion behavior at the transition can be measured by cryogenic magnetic sensors. At the present state, the cryostat is equipped with fluxgates and a first prototype of AMR sensor with its own calibration circuitry. A magnetic field mapping system integrating several AMR sensors is currently under development. All the sensors output will be digitized with a purpose-made evaluation board to be installed inside the cryostat. The Helmoltz coil setup will also be employed to calibrate at cold the AMR sensors, whose sensitivity is expected to change with temperature [14], and to evaluate flux expulsion characteristics of the cavity as function of cooldown rate and temperature gradient at the transition temperature.

Additionally, a fully digital and FPGA-based Phase-Locked Loop (PLL) systemis currently being developed to replace the analog cavity control system. This new control crate, similar to the ones developed at UKRI or Fermilab, will integrate with high flexibility, seamlessly operating across different frequencies. It will also simplify the harmonization of cavity control and test data acquisition across various laboratories within the PIP-II collaboration.

CONCLUSIONS

This manuscript presents the recent activities carried out by LASA-INFN towards the series production of PIP-II LB650 cavities. These activities primarily involved the development of single and multi-cell cavity prototypes to establish the processing recipe within an industrial context. In addition to defining the cavity surface treatments, LASA-

ISBN: 978-3-95450-234-9 ISSN: 2673-5504 doi:10.18429/JACoW-SRF2023-TUPTB059

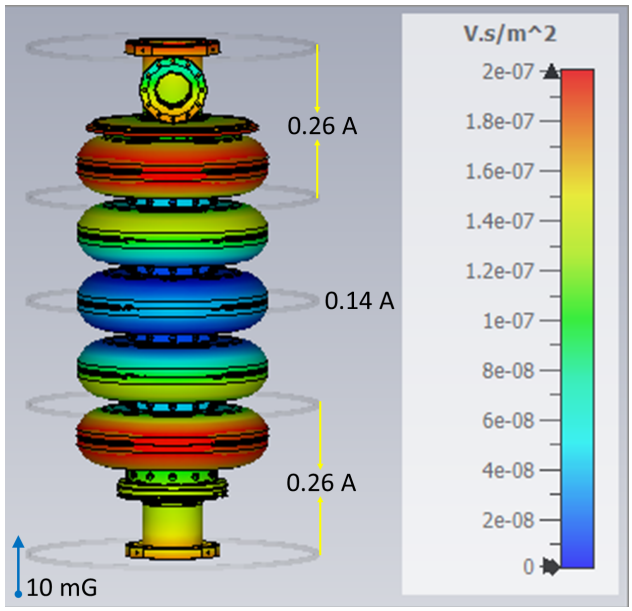

Figure 6: Residual magnetic field along cavity surface employing 2 Helmholtz coils and a single central coil after parametric optimization for a residual field of 10 mG. The coil currents are also indicated.

INFN is also making preparations for the upcoming series production phase. This includes finalizing the configuration for cavity testing and refining the vertical test strategy.

With the objective of testing high-Q cavities, the LASA-INFN facility is undergoing upgrades to minimize residual resistance caused by trapped magnetic flux. This upgraded facility will serve as a backup solution for testing undressed LB650 cavities if needed and will also enable a thorough analysis of the magnetic expulsion characteristics of the cavities under investigation.

REFERENCES

[1] PIP-II Preliminary Design Report, Revision of March 22nd, 2019, as presented at PIP-II MAC, Mar. 25th, 2019

[2] R. Paparella *et al.*, "INFN-LASA for the PIP-II Project", in *Proc. SRF'19*, Dresden, Germany, Jun.-Jul. 2019, pp. 205–209. doi:10.18429/JACoW-SRF2019-MOP060

[3] M. Martinello *et al.*, "Q-factor optimization for high-beta 650 MHz cavities for PIP-II", *J. Appl. Phys.*, vol. 130, p. 174501, 2021. doi:10.1063/5.0068531

[4] M. Bertucci *et al.*, "Electropolishing of PIP-II Low Beta Cavity Prototypes", in *Proc. SRF'19*, Dresden, Germany, Jun.-Jul. 2019, pp. 194–198. doi:10.18429/JACoW-SRF2019-MOP057

[5] M. Bertucci *et al.*, "Status of LASA-INFN R&D Activity on PIP-II Low-beta Prototypes", in *Proc. IPAC'22*, Bangkok, Thailand, Jun. 2022, pp. 1241–1244. doi:10.18429/JACoW-IPAC2022-TUPOTK020

[6] A. Romanenko, F. Barkov, L. Cooley, and A. Grassellino, "Proximity breakdown of hydrides in superconducting niobium cavities", *Supercond. Sci. Technol.*, vol. 26, p. 014024, 2012. doi:10.1088/0953-2048/26/3/035003

[7] W. Singer *et al.*, "Production of superconducting 1.3-GHz cavities for the European X-ray Free Electron Laser", *Phys. Rev. Accel. Beams*, vol. 19, p. 092001, 2016. doi:10.1103/PhysRevAccelBeams.19.092001

[8] H. Ito, H. Araki, K. Takahashi, and K. Umemori, "Influence of furnace baking on Q–E behavior of superconducting accelerating cavities", *Prog. Theor. Exp. Phys.*, vol. 2021, no. 7, p. 071G01. doi:10.1093/ptep/ptab056

[9] P. Sha *et al.*, "Quality Factor Enhancement of 650 MHz Superconducting Radio-Frequency Cavity for CEPC", *Appl. Sci.*, vol. 12, p. 546, 2022. doi:10.3390/app12020546

[10] V. Chouhan *et al.*, "Study on Electropolishing Conditions for 650 MHz Niobium SRF Cavity", in *Proc. NAPAC'22*, Albuquerque, NM, USA, Aug. 2022, pp. 97–99. doi:10.18429/JACoW-NAPAC2022-MOPA22

[11] L. Monaco *et al.*, "Fabrication and Treatment of the ESS Medium Beta Prototype Cavities", in *Proc. IPAC'17*, Copenhagen, Denmark, May 2017, pp. 1003–1006. doi:10.18429/JACoW-IPAC2017-MOPVA060

[12] D. Sertore *et al.*, "Recent Update on ESS Medium Beta Cavities at INFN LASA", in *Proc. IPAC'22*, Bangkok, Thailand, Jun. 2022, pp. 1245–1248. doi:10.18429/JACoW-IPAC2022-TUPOTK021

[13] M. Bertucci *et al.*, "Upgrade on the Experimental Activities for ESS at the LASA Vertical Test Facility", in *Proc. SRF'19*, Dresden, Germany, Jun.-Jul. 2019, pp. 1133–1138. doi:10.18429/JACoW-SRF2019-THP093

[14] J. C. Wolff *et al.*, "Development of a New B-Mapping System for SRF Cavity Vertical Tests", in *Proc. SRF'21*, East Lansing, MI, USA, Jun.-Jul. 2021, pp. 137. doi:10.18429/JACoW-SRF2021-SUPTEV009